Title
Cell type specific tracing of the subcortical input to primary visual cortex from the basal forebrain

Journal
The Journal of Comparative Neurology, 527(3)

ISSN
1550-7149

Authors
Lean, Georgina A
Liu, Yong-Jun
Lyon, David C

Publication Date
2019-02-15

DOI
10.1002/cne.24412

Peer reviewed

Published in final edited form as:

J Comp Neurol. 2019 February 15; 527(3): 589–599. doi:10.1002/cne.24412.

Cell type specific tracing of the subcortical input to primary visual cortex from the basal forebrain

Georgina A. Lean[1,2], **Yong-jun Liu**[2,a], and **David C. Lyon**[2,*]

[1]Department of Cognitive Sciences, School of Social Sciences, University of California, Irvine, CA 92697, USA

[2]Department of Anatomy & Neurobiology, School of Medicine, University of California, Irvine, CA 92697, USA

Abstract

The basal forebrain provides cholinergic inputs to primary visual cortex (V1) that play a key modulatory role on visual function. While basal forebrain afferents terminate in the infragranular layers of V1, acetylcholine is delivered to more superficial layers through volume transmission. Nevertheless, direct synaptic contact in deep layers 5 and 6 may provide a more immediate effect on V1 modulation. Using helper viruses with cell type specific promoters to target retrograde infection of pseudotyped and genetically modified rabies virus evidence was found for direct synaptic input onto V1 inhibitory neurons. These inputs were similar in number to geniculocortical inputs and, therefore, considered robust. In contrast, while clear evidence for LGN input to V1 excitatory neurons was found, there was no evidence of direct synaptic input from the basal forebrain. These results suggest a direct and more immediate influence of the basal forebrain on local V1 inhibition.

Keywords

Acetylcholine; Basal forebrain; Cholinergic; Cortical inhibition; Cortical layers; Diagonal band; GABAergic; inhibitory neurons; subcortical; V1; Visual Cortex V1; RRID:AB_477652; RRID:AB_523902

Visual perception occurs through a complex network of cortical processing that relies on driving, modulating, and integrating interconnectivity with subcortical visual structures as studied extensively in rodents (Guillery and Sherman, 2002; Krubitzer et al., 2011; Marshel et al., 2011; Niell, 2015; Negwer et al., 2017; Seabrook et al., 2017), carnivores (Reid and Alonso, 1995; Liu et al., 2011; Hashemi-Nezhad and Lyon, 2012) non-human primates (Felleman and Van Essen, 1991; Casagrande, 1994; Lyon et al., 2002; Casagrande et al., 2005; Kaas, 2012), and close relatives such as the tree shrew (Casagrande and Harting, 1975; Lyon et al., 1998; Casagrande et al., 2002). The lateral geniculate nucleus, the

[*]**Corresponding Author:** David C. Lyon, 364 Med Surge II, University of California, Irvine, CA 92697-1275, Phone: 949-824-0447, Fax: 949-824-8549, dclyon@uci.edu.

[a]**Current Address:** Department of Honeybee Protection and Biosafety, Institute of Apicultural Research, Chinese Academy of Agricultural Sciences, No.1 Beigou Xiangshan, Haidian District, Beijing, 100093, People's Republic of China

Guest Editor: Jon H. Kaas

superior colliculus and the pulvinar nucleus, are among the most studied subcortical visual regions, having been subject to decades of anatomical and functional investigation by Vivien Casagrande and her colleagues in tree shrew (i.e., Casagrande et al., 1972; Lyon et al., 2003a; Lyon et al., 2003b; Vanni et al., 2015) and primate (i.e.,Fitzpatrick et al., 1980; Lachica and Casagrande, 1992; Stepniewska and Kaas, 1997; Xu et al., 2001; Nassi et al., 2006; Imura and Rockland, 2007; Kaas and Lyon, 2007; Lyon et al., 2010; Purushothaman et al., 2012; Cerkevich et al., 2014;), and by many others in rodent (i.e., Lysakowski et al., 1986; Sanderson et al., 1991; Van Hooser and Nelson, 2006; Marshel et al., 2012; Cruz-Martin et al., 2014; Tohmi et al., 2014; Roth et al., 2016; Seabrook et al., 2017; Zhou et al., 2017; Zhou et al., 2018).

Another subcortical region, the basal forebrain, has also long been known to provide input to visual cortex (Figure 1a; Henderson, 1981; Tigges et al., 1982; Carey & Rieck, 1987; Dreher et al, 1990); however, the functional contribution of this input is only starting to become understood (i.e., Goard and Dan, 2009; Newman et al., 2012; Pinto et al., 2013). The basal forebrain output to cortex is predominantly characterized as cholinergic (Henderson, 1981; Sarter et al., 2005; Pinto et al., 2013). Given the high density of cholinergic varicosities and receptors within V1 (Lysakowski et al., 1989; Mechawar et al., 2000; Wong and Kaas, 2008; Wong and Kaas, 2010; Disney and Reynolds, 2014) and the functional contribution of acetylcholine to receptive field tuning, attentional modulation, and plasticity in V1 (Sillito and Kemp, 1983; Bear and Singer, 1986; Roberts et al., 2005; Herrero et al., 2008; Newman et al., 2012; Avery et al., 2014), the basal forebrain is particularly well-suited to influence V1 processing (Chubykin et al., 2013; Pinto et al., 2013).

Acetylcholine from the basal forebrain is delivered to V1 across most cortical layers via diffuse extra-synaptic modulation known as ‘volume transmission’ (Descarries et al., 1997; Sarter et al., 2009). This is reinforced by anatomical evidence showing acetylcholine receptors evenly distributed across layers 2–6 (Disney et al., 2006; 2014). In layers 2/3, 5 and 6, cholinergic receptors are found predominantly on inhibitory neurons leading to GABAergic mediated suppression (Disney et al., 2006; Disney et al., 2007; Disney et al., 2012; 2014). Furthermore, basal forebrain afferents terminate exclusively within infragranular layers 5 and 6 (Figure 1b; Carey and Rieck, 1987; Rieck and Carey, 1984). Therefore, unlike superficial cortical layers, the effect on neurons in layers 5 and 6 can be more immediate.

Based on the preponderance of cholinergic receptors being found on inhibitory neurons (Disney et al., 2006; 2014) one might expect direct synaptic basal forebrain inputs to primarily contact inhibitory neurons. To determine this, we took advantage of our recently developed technique (Liu et al., 2013), where a helper virus containing either a GAD1 or an αCamKII promoter is used to target a genetically modified rabies virus (Wickersham et al., 2007) for retrograde tracing of the direct inputs to either inhibitory or excitatory V1 neurons, respectively (Figure 2). In this way we are able to determine whether or not there is a difference in direct synaptic inputs of the basal forebrain to inhibitory and excitatory neurons.

MATERIALS AND METHODS

Surgical Procedures

Eighteen adult C57BL/6 mice of both sexes were used following procedures approved by the University of California, Irvine Institutional Animal Care and Use Committee and the Institutional Biosafety Committee, and the guidelines of the National Institutes of Health were followed.

Six mice were given 9 injections of the mCherry (mCh) and/or green fluorescent protein (GFP) versions of the glycoprotein-deleted rabies virus (ΔG-RV; Table 1). Twelve different mice were given injections of a helper virus (AAV-GAD1-YTB or LV-αCamKII-YTB; Table 2). Anesthesia was induced and maintained with isoflurane throughout the procedure. Once anesthetized animals were placed in a stereotaxic head-holder and a craniotomy was performed over the caudal half of neocortex under sterile conditions. Glass pipettes with tips broken to approximately 20 μm were filled with virus and inserted through dura using a computer-controlled micro-positioner attached to a KOPF stereotaxic arm. Coordinates between 3.0–4.5 mm posterior from Bregma and 1.25–3.25 mm lateral to the midline were used. ΔG-RV injections were made at a depth of ~500 μm and a volume of ~0.3 μl. For AAV and LV helper viruses, ~0.5 μl injections were made in a single V1 location at a cortical depth between 400–600 μm. After injection, artificial dura (Tecoflex, Microspec Corp.) was placed over the craniotomy, the skull sealed with dental acrylic, and the animals revived. Mice injected with ΔG-RV were given a 7–10 day survival time and then perfused for histology.

Mice injected with helper virus were given a 3 week survival period followed by an intracranial injection of EnvA-ΔG-RV (see Figure 2 for injection timeline). For EnvA-ΔG-RV injections each animal was anesthetized as before, and under sterile conditions the acrylic skull cap removed and EnvA injections of ~0.5 μl made as close as possible to the original helper virus injected location based on the coordinates and landmarks described above. The craniotomy was then covered with fresh Tecoflex, resealed with dental acrylic, and the animals revived. A final survival period ranging from 7–10 days followed.

Viruses

The ΔG-RV expressing either mCherry or GFP, and the EnvA-ΔG-RV expressing mCherry were produced and concentrated following protocols described previously (Wickersham et al., 2007; Wickersham et al.., 2010; Osakada et al., 2011) a titer range if of ~5×10^9 infectious units/ml.

For helper viruses, GAD1-YTB (7,382 bp) and αCamKII-YTB (7,500 bp) were sublconed into adeno-associated virus (AAV) and lentiviral (LV) backbones to make AAV-GAD1-YTB (11.0 kb) and LV-αCamKII-YTB (12.3 kb), as described previously (Liu et al., 2013). From these plasmids, serotype 9 AAV and VSV-G pseudotyped LV particles were prepared and purified by the Gene Transfer Targeting and Therapeutics Core at the Salk Institute of Biological Studies (La Jolla, CA) yielding a titer of 9×10^9 genome copies/ml for AAV and 2×10^{10} transducing units/ml for LV.

Histology and Antibody Reporting

For histology, animals were deeply anesthetized with Euthasol and perfused transcardially, first with saline, then followed by 4% paraformaldehyde in phosphate buffer (PB; pH 7.4). For most animals, 1.5% glutaraldehyde was also included. Brains were removed and cryoprotected in 30% sucrose for ~48 hours prior to sectioning.

Brains were cut coronally at 30 μm up to 1 mm posterior and anterior to the V1 injection site, and at 40 μm elsewhere. A series of every fourth 30 μm section was processed for GABA using the anti-GABA rabbit polyclonal antibody (1:200; Sigma-Aldrich Cat# A2052, RRID:AB_477652; tested in GABA expressing cells isolated from the pallium in mice; conjugated to BSA). Immunopositive neurons were revealed using the fluorescent secondary Alexa Fluor 350 goat anti-rabbit IgG (1:500; Invitrogen). To enhance visualization of YFP the same sections were also processed for the anti-GFP chicken polyclonal antibody (1:1000; Novus Cat# NB 100–1614, RRID:AB_523902; tested on transgenic mice expressing recombinant GFP; Immunogen affinity purified) and revealed using Alexa Fluor 488 goat anti-rabbit IgG (1:500; Invitrogen). The mCherry and GFP reporters from rabies virus were not enhanced through immunofluorescence. One to two additional series of every fourth section were processed instead for DAPI. Rabies virus infected neurons could be visualized in all sections without processing. Sections were mounted in PVA-DABCO (Sigma-Aldrich) to preserve fluorescence.

Data Analysis

Sections were examined using fluorescent microscopy (Zeiss Axioplan) with 10× (0.45 NA) and 20× (0.8 NA) objectives and cell positions reconstructed using Neurolucida software (MicroBrightField, Williston, VT) off-line. To limit bleaching of fluorescence, images of whole sections were captured with a high-power black and white digital camera (Cooke SensiCam QE) and stitched together through the Virtual Slide module.

For each case, two or three of every four sections were used to identify the number and laminar location of starter cells in V1 and rabies infected neurons in the LGN and diagonal band of the basal forebrain. Interpolated cell-counts were generated for Tables 1 and 2 by multiplying the number of cells by 2 for cases where 2 out of 4 sections were examined, or multiplying by 1.33 for cases where 3 out of every 4 sections were used.

Confirmation of V1 injection sites and the locations of the LGN and diagonal band were based on the atlas by Paxinos and Franklin (2001).

Results

Using injections of cell type specific viral tracers in V1, we found that neurons in the basal forebrain project directly to V1 inhibitory neurons, but found no evidence for direct projections to cortical excitatory neurons. We also found the basal cortical projections to be similar in number to LGN inputs to V1.

ΔG-RV retrograde infection of basal forebrain

Prior to using the cell type specific helper viruses to target EnvA-ΔG-RV, we first made injections of ΔG-RV. The ΔG-RV version of rabies virus acts as a monosynaptic retrograde tracer and does not require a helper virus (Wickersham et al., 2007; Connolly et al., 2012). While this virus cannot distinguish between inputs to inhibitory and excitatory neurons, the goal of these injections was to determine the ability and degree to which rabies virus infects basal forebrain neurons targeting V1 by comparing to the number of infected neurons in the LGN.

Nine distinct injections of ΔG-RV with either the mCherry or GFP reporter were made into V1 of 6 mice (Table 1). All 9 injections resulted in labeled neurons in the diagonal band of the basal forebrain and the LGN, with the average for basal forebrain (13.4±4.9) about two thirds that of the number of neurons found in the LGN (21.3±6.5).

An example of two injections in the same animal is shown in Figure 3a. Based on the density of intrinsic V1 labeled neurons, the injection sites reached layers 4, 5, and 6 which would be necessary to target axon terminals from LGN and basal forebrain neurons. A reconstruction of the pattern of labeled cells from an injection in a second case is shown in Figure 4a. As in the digital image in Figure 3a, the reconstruction of posterior sections 45 and 50 shows that the V1 injection site extended through layers 4, 5, and 6. Expected inter-areal connections with other visual cortical areas were observed, along with a cluster of neurons in the LGN. In more anterior sections (102, 109, and 115) clusters of basal forebrain neurons are shown ventral medially, along with a few labeled neurons in cingulate cortex dorsal medially, and the claustrum laterally. Digital images show that labeled diagonal band neurons had a distinct large soma size and long spiny dendrites (Figure 4c–d). Compared to basal forebrain neurons, LGN neurons were packed together more tightly with smaller somas and shorter dendrites (Figure 4b).

AAV-GAD1-YTB targeted retrograde tracing with EnvA-ΔG-RV

To determine whether basal forebrain neurons project to V1 inhibitory neurons we made injections of the helper virus, AAV-GAD1-YTB, to target infection of the retrograde EnvA-ΔG-RV to inhibitory neurons. Injections were made into a single V1 hemisphere of 6 mice (Table 2). In five of six cases, retrograde infected neurons were found in the diagonal band of the basal forebrain, averaging 8±3.4 per case. Five cases also yielded labeled neurons in the LGN with and average number of 13±5.1.

An injection site example is shown from one case in Figure 3d–h. YFP expressing neurons (Figure 3f) were confirmed as inhibitory through co-labeling with the GABA antibody (Figure 3h). Rabies virus infected neurons expressed mCherry (Figure 3g). Starter cells in V1 were defined as neurons co-expressing YFP and mCherry (yellow neurons in Figure 3e); Neurons expressing mCherry only were defined as presynaptically connected neurons. Starter cells were evident throughout layers 4, 5 and 6 (see also Table 2).

A reconstruction of the distribution of inputs to V1 inhibitory starter cells is shown in a second case (Figure 5a). Starter cells were distributed throughout all layers as shown in section 76, with presynaptically connected neurons found in the LGN in section 80 (Figure

5b) and in the diagonal band of the basal forebrain (Figure 5c–e) as shown in the three most anterior sections. Overall, a nearly equal number of starter cells were present in layer 5 and 6, and a nearly equal number of presynaptic neurons were labeled in the diagonal band and LGN (Table 2).

LV-αCamKII-YTB targeted retrograde tracing with EnvA-ΔG-RV

To determine whether basal forebrain neurons project to V1 excitatory neurons we made injections of the lentiviral vector, LV-αCamKII-YTB, to target infection of the retrograde EnvA-ΔG-RV to excitatory neurons. Injections were made into a single V1 hemisphere of 6 mice (Table 2). In five of six cases (Table 2), retrograde infected neurons were found in the LGN (6.4±1.7 per case). However, no infected neurons were found in the basal forebrain.

An injection site example is shown from one case in Figure 3i–m. YFP expressing neurons (Figure 3k) were confirmed as excitatory for not co-labeling with the GABA antibody (Figure 3m). Rabies virus infected neurons expressed mCherry (Figure 3l). Starter cells in V1 were defined as neurons co-expressing YFP and mCherry (yellow neurons in Figure 3j); Neurons expressing mCherry only were defined as presynaptically connected neurons. Yellow starter cells were evident throughout layers 4, 5 and 6 (Figure 3i; see also Table 2).

A reconstruction of the distribution of inputs to V1 excitatory starter cells is shown in a second case (Figure 6a). In the posterior most section, starter cells were distributed throughout layers 4, 5 and 6, with presynaptically connected neurons found in the LGN in section 70 (Figure 6b). Presynaptically infected neurons were labeled as far posterior as the cingulate cortex (Cg), but no cells were found in the basal forebrain.

Discussion

The goal of this present experiment was to determine the cell type specific nature of projections from the basal forebrain to primary visual cortex. Using a dual viral retrograde tracing method we found evidence for direct synaptic input to inhibitory neurons. These inputs were robust as they were similar in number to geniculocortical inputs to inhibitory neurons. In contrast, we found clear evidence for LGN input to V1 excitatory neurons, but no evidence for direct synaptic input from the basal forebrain. Taken into consideration with other evidence discussed below, our results indicate a strong direct influence of the basal forebrain on local V1 inhibition.

We previously demonstrated the cell type specificity of AAV-GAD1 and LV-αCamKII on cortical inhibitory and excitatory neurons, and showed that the delivery of YTB through these helper viruses was sufficient to label presynaptic inputs throughout the brain, with an emphasis on intrinsic V1 connectivity (Liu et al., 2013). Here we re-confirmed the cell type specificity of each helper virus and found differences in the basal forebrain inputs to V1.

The observed projection of basal forebrain to inhibitory, but not excitatory V1 neurons was not likely due to differences in the two helper viruses used. On the contrary, viral vectors were optimized for their endogenous neurotropism; lentivirus for excitatory neurons and low-titer AAV for inhibitory neurons (Nathanson, 2009). Moreover, both helper viruses

resulted in retrogradely infected neurons in the LGN; the LGN provided input to both inhibitory and excitatory V1 neurons. Demonstrating that the AAV and lentiviral vectors were both effective at initiating cell type specific retrograde tracing of EnvA-ΔG-RV.

Because previous reports found that only deep V1 injections provided retrograde labeling of basal forebrain neurons (Carey and Rieck, 1987; Rieck and Carey, 1984). We also targeted infragranular layers with our viruses. No discernable difference was found between the distribution of inhibitory and excitatory starter cells in layers 5 and 6.

While no basal forebrain neurons were found to project to excitatory V1 cells. This does not necessarily mean that this connection is not present. Our method of complementation of EnvA-ΔG-RV with the B19 strain of the rabies glycoprotein (B from YTB) is most likely to label stronger connections, based on the number of synaptic inputs (Liu et al., 2013; also see Lyon et al., 2010; Lyon and Rabideau, 2012; Liu et al., 2014). Therefore, it is possible for weaker connections to be missed. In support of this, a slight loss in the average number of basal forebrain and LGN cells labeled by helper virus complementation of EnvA-ΔG-RV, was observed compared to ΔG-RV, which does not require complementation (compare Tables 1 and 2). In addition, studies using transgenic mice to provide higher levels of the rabies glycoprotein did show a basal forebrain input to three types of V1 excitatory neurons (Kim et al., 2015).

A stronger or exclusive direct synaptic input to infragranular inhibitory neurons as our results suggest, is consistent with other work indicating a greater effect of the cholinergic system on inhibition in V1. While an excitatory effect of acetylcholine has been observed, this is likely most predominant in layer 4 where there is an abundance of nicotinic receptors found on excitatory neurons (Disney et al., 2007). However, in layers 2/3, 5 and 6, M1 and M2 type muscarinic receptors are found predominantly on inhibitory neurons, despite inhibitory neurons only representing ~20% of the V1 neural population (Disney et al., 2006; Disney et al., 2007; Disney et al., 2012). Consistent with this anatomy, in layers 2/3, 5 and 6, acetylcholine largely leads to suppressed V1 cell activity (Disney et al., 2012). Moreover, in layer 5 acetylcholine release was shown to amplify the inhibitory signal and decreases the excitability and sensory responsiveness of pyramidal neurons (Lucas-Meunier et al., 2009). This inhibitory effect could result from direct synaptic contact onto local deep layer inhibitory neurons, which in turn suppress neighboring excitatory pyramidal cells.

Acknowledgments

We thank Drs. Markus Ehrengruber and Han-Juan Shao for assistance with preparation of viruses. This work was supported in part by grants from the Whitehall Foundation (#2009-12-44 and #2014-08-100), the National Institute of Neurological Disorders and Stroke (R21NS072948) and the National Eye Institute (R01EY024890).

This work was supported by the Whitehall Foundation (#2009-12-44 and #2014-08-100), the National Institute of Neurological Disorders and Stroke (R21NS072948) and the National Eye Institute (R01EY024890).

List of Abbreviations

αCamKII	Alpha Ca2+/calmodulin-dependent kinase II
ΔG	Glycoprotein-deleted

AAV	Adeno-associated virus
aca	Anterior commissure, anterior part
acp	Anterior commissure, posterior part
AV	Anteroventral thalamic nucleus
BF	Basal forebrain
BSTS	Bed nucleus of the stria terminalis, supracapsular part
Cg	Cingulate cortex
Cl	Claustrum
Cpu	Caudate and putamen
DB	Diagonal band of the basal forebrain
EnvA	Envelope A glycoprotein
f	Fornix
GABA	Gamma-aminobutyric acid
GAD1	Glutamate decarboxylase 1
GFP	Green fluorescent protein
ic	Internal capsule
L1	Cortical layer 1
L2/3	Cortical layer 2 and 3
L4	Cortical layer 4
L5	Cortical layer 5
L6	Cortical layer 6
LGN	Dorsal lateral geniculate nucleus
LGp	Lateral globus pallidus
LP	Lateral posterior nucleus (pulvinar)
LV	Lentivirus
mCherry	Red fluorescent protein
PVA-DABCO	Polyvinyl alcohol mounting medium with 1,4-diazabicyclo[2.2.2]octane
RabG	B19 strain of the rabies glycoprotein

RV	Rabies virus
TS	Triangular septal nucleus
V1	Primary visual cortex
V2L	Second visual area, lateral
V2M	Second visual area, medial
VSV-G	Vesicular stomatitis virus glycoprotein
YFP	Yellow fluorescent protein
YTB	YFB, TVA receptor, B19 strain of rabies glycoprotein

References

Avery MC, Dutt N, Krichmar JL. 2014; Mechanisms underlying the basal forebrain enhancement of top-down and bottom-up attention. Eur J Neurosci. 39:852–65. [PubMed: 24304003]

Bear MF, Singer W. 1986; Modulation of visual cortical plasticity by acetylcholine and noradrenaline. Nature. 320:172–176. [PubMed: 3005879]

Carey RG, Rieck RW. 1987; Topographic projections to the visual cortex from the basal forebrain in the rat. Brain Res. 424:205–15. [PubMed: 2823995]

Casagrande VA. 1994; A third parallel visual pathway to primate area V1. Trends Neurosci. 17:305–10. [PubMed: 7524217]

Casagrande VA, Harting JK. 1975; Transneuronal transport of tritiated fucose and proline in the visual pathways of tree shrew Tupaia glis. Brain Res. 96:367–72. [PubMed: 809113]

Casagrande VA, Harting JK, Hall WC, Diamond IT, Martin GF. 1972; Superior colliculus of the tree shrew: a structural and functional subdivision into superficial and deep layers. Science. 177:444–7. [PubMed: 5043147]

Casagrande VA, Joseph R. 1980; Morphological effects of monocular deprivation and recovery on the dorsal lateral geniculate nucleus in galago. J Comp Neurol. 194:413–426. [PubMed: 7440808]

Casagrande VA, Sáry G, Royal D, Ruiz O. 2005; On the impact of attention and motor planning on the lateral geniculate nucleus. Prog Brain Res. 149:11–29. [PubMed: 16226573]

Casagrande VA, Xu X, Sáry G. 2002; Static and dynamic views of visual cortical organization. Prog Brain Res. 136:389–408. [PubMed: 12143396]

Cerkevich C, Lyon D, Balaram P, Kaas J. 2014; Distribution of cortical neurons projecting to the superior colliculus in macaque monkeys. Eye Brain. 2014:121. [PubMed: 25663799]

Chubykin AA, Roach EB, Bear MF, Shuler MGH. 2013; A cholinergic mechanism for reward timing within primary visual cortex. Neuron. 77:723–735. [PubMed: 23439124]

Clay Reid R, Alonso J-M. 1995; Specificity of monosynaptic connections from thalamus to visual cortex. Nature. 378:281–284. [PubMed: 7477347]

Connolly Jason D, Hashemi-Nezhad M, Lyon DC. 2012; Parallel feedback pathways in visual cortex of cats revealed through a modified rabies virus. J Comp Neurol. 520:988–1004. [PubMed: 21826663]

Cruz-Martín A, El-Danaf RN, Osakada F, Sriram B, Dhande OS, Nguyen PL, Callaway EM, Ghosh A, Huberman AD. 2014; A dedicated circuit links direction-selective retinal ganglion cells to the primary visual cortex. Nature. 507:358–361. [PubMed: 24572358]

Descarries L, Gisiger V, Steriade M. 1997; Diffuse transmission by acetylcholine in the CNS. Prog Neurobiol. 53:603–25. [PubMed: 9421837]

Disney AA, Aoki C, Hawken MJ. 2007; Gain modulation by nicotine in macaque V1. Neuron. 56:701–713. [PubMed: 18031686]

Disney AA, Reynolds JH. 2014; Expression of m1-type muscarinic acetylcholine receptors by parvalbumin-immunoreactive neurons in the primary visual cortex: A comparative study of rat, guinea pig, ferret, macaque, and human. J Comp Neurol. 522:986–1003. [PubMed: 23983014]

Disney AA, Aoki C, Hawken MJ. 2012; Cholinergic suppression of visual responses in primate V1 is mediated by GABAergic inhibition. J Neurophysiol. 108:1907–23. [PubMed: 22786955]

Disney AA, Domakonda KV, Aoki C. 2006; Differential expression of muscarinic acetylcholine receptors across excitatory and inhibitory cells in visual cortical areas V1 and V2 of the macaque monkey. J Comp Neurol. 499:49–63. [PubMed: 16958109]

Dreher B, Dehay C, Bullier J. 1990; Bihemispheric Collateralization of the Cortical and Subcortical Afferents to the Rat's Visual Cortex. Eur J Neurosci. 2:317–331. [PubMed: 12106039]

Felleman DJ, Van Essen DC. 1991; Distributed hierarchical processing in the primate cerebral cortex. Cereb Cortex. 1:1–47. [PubMed: 1822724]

Fitzpatrick D, Carey RG, Diamond IT. 1980; The projection of the superior colliculus upon the lateral geniculate body in Tupaia glis and Galago senegalensis. Brain Res. 194:494–9. [PubMed: 7388626]

Goard M, Dan Y. 2009; Basal forebrain activation enhances cortical coding of natural scenes. Nat Neurosci. 12:1444–1449. [PubMed: 19801988]

Guillery RW, Sherman SM. 2002; Thalamic relay functions and their role in corticocortical communication: generalizations from the visual system. Neuron. 33:163–75. [PubMed: 11804565]

Hashemi-Nezhad M, Lyon DC. 2012; Orientation Tuning of the Suppressive Extraclassical Surround Depends on Intrinsic Organization of V1. Cereb cortex. 22:308–326. [PubMed: 21666124]

Henderson Z. 1981; A projection from acetylcholinesterase-containing neurones in the diagonal band to the occipital cortex of the rat. Neuroscience. 6:1081–1088. [PubMed: 7279215]

Herrero JL, Roberts MJ, Delicato LS, Gieselmann MA, Dayan P, Thiele A. 2008; Acetylcholine contributes through muscarinic receptors to attentional modulation in V1. Nature. 454:1110–1114. [PubMed: 18633352]

Imura K, Rockland KS. 2006; Long-range interneurons within the medial pulvinar nucleus of macaque monkeys. J Comp Neurol. 498:649–666. [PubMed: 16917851]

Kaas JH. 2012; Evolution of columns, modules, and domains in the neocortex of primates. Proc Natl Acad Sci. 109:10655–10660. [PubMed: 22723351]

Kaas JH, Lyon DC. 2007; Pulvinar contributions to the dorsal and ventral streams of visual processing in primates. Brain Res Rev. 55:285–96. [PubMed: 17433837]

Kim EJ, Jacobs MW, Ito-Cole T, Callaway EM. 2016; Improved monosynaptic neural circuit tracing using engineered rabies virus glycoproteins. Cell Reports. 15:692–699. [PubMed: 27149846]

Krubitzer L, Campi KL, Cooke DF. 2011; All rodents are not the same: a modern synthesis of cortical organization. Brain Behav Evol. 78:51–93. [PubMed: 21701141]

Lachica EA, Casagrande VA. 1992; Direct W-like geniculate projections to the cytochrome oxidase (CO) blobs in primate visual cortex: Axon morphology. J Comp Neurol. 319:141–158. [PubMed: 1375606]

Liu Y-J, Hashemi-Nezhad M, Lyon DC. 2011; Dynamics of extraclassical surround modulation in three types of V1 neurons. J Neurophysiol. 105:1306–17. [PubMed: 21228302]

Liu Y-J, Ehrengruber MU, Negwer M, Shao H-J, Cetin AH, Lyon DC. 2013; Tracing inputs to inhibitory or excitatory neurons of mouse and cat visual cortex with a targeted rabies virus. Curr Biol. 23:1746–1755. [PubMed: 23993841]

Liu Y, Arreola M, Coleman C, Lyon D. 2014; Very-long-range disynaptic V1 connections through layer 6 pyramidal neurons revealed by transneuronal tracing with rabies virus. Eye Brain. 6:45–56. [PubMed: 28539788]

Lucas-Meunier E, Monier C, Amar M, Baux G, Fregnac Y, Fossier P. 2009; Involvement of nicotinic and muscarinic receptors in the endogenous cholinergic modulation of the balance between excitation and inhibition in the young rat visual cortex. Cereb Cortex. 19:2411–2427. [PubMed: 19176636]

Lyon DC, Jain N, Kaas JH. 2003; The visual pulvinar in tree shrews II. Projections of four nuclei to areas of visual cortex. J Comp Neurol. 467:607–27. [PubMed: 14624492]

Lyon DC, Jain N, Kaas JH. 2003; The visual pulvinar in tree shrews I. Multiple subdivisions revealed through acetylcholinesterase and Cat-301 chemoarchitecture. J Comp Neurol. 467:593–606. [PubMed: 14624491]

Lyon DC, Nassi JJ, Callaway EM. 2010; A disynaptic relay from superior colliculus to dorsal stream visual cortex in macaque monkey. Neuron. 65:270–9. [PubMed: 20152132]

Lyon DC, Rabideau C. 2012; Lack of robust LGN label following transneuronal rabies virus injections into macaque area V4. J Comp Neurol. 520:2500–11. [PubMed: 22237967]

Lyon DC, Xu X, Casagrande Va, Stefansic JD, Shima D, Kaas JH. 2002; Optical imaging reveals retinotopic organization of dorsal V3 in New World owl monkeys. Proc Natl Acad Sci U S A. 99:15735–42. [PubMed: 12441399]

Lysakowski A, Wainer BH, Bruce G, Hersh LB. 1989; An atlas of the regional and laminar distribution of choline acetyltransferase immunoreactivity in rat cerebral cortex. Neuroscience. 28:291–336. [PubMed: 2646551]

Lysakowski A, Standage GP, Benevento LA. 1986; Histochemical and architectonic differentiation of zones of pretectal and collicular inputs to the pulvinar and dorsal lateral geniculate nuclei in the macaque. J Comp Neurol. 250:431–448. [PubMed: 3760248]

Marshel JH, Garrett ME, Nauhaus I, Callaway EM. 2011; Functional Specialization of Seven Mouse Visual Cortical Areas. Neuron. 72:1040–1054. [PubMed: 22196338]

Mechawar N, Cozzari C, Descarries L. 2000; Cholinergic innervation in adult rat cerebral cortex: a quantitative immunocytochemical description. J Comp Neurol. 428:305–18. [PubMed: 11064369]

Nathanson JL, Yanagawa Y, Obata K, Callaway EM. 2009; Preferential labeling of inhibitory and excitatory cortical neurons by endogenous tropism of adeno-associated virus and lentivirus vectors. Neuroscience. 161:441–50. [PubMed: 19318117]

Nassi JJ, Lyon DC, Callaway EM. 2006; The parvocellular LGN provides a robust disynaptic input to the visual motion area MT. Neuron. 50:319–27. [PubMed: 16630841]

Negwer M, Liu YJ, Schubert D, Lyon DC. 2017; V1 connections reveal a series of elongated higher visual areas in the California ground squirrel, Otospermophilus beecheyi. J Comp Neurol. 525:1909–1921. [PubMed: 28078786]

Newman EL, Gupta K, Climer JR, Monaghan CK, Hasselmo ME. 2012; Cholinergic modulation of cognitive processing: insights drawn from computational models. Front Behav Neurosci. 6:1–19. [PubMed: 22279431]

Niell CM. 2015; Cell Types, Circuits, and Receptive Fields in the Mouse Visual Cortex. Annu Rev Neurosci. 38:413–431. [PubMed: 25938727]

Paxinos, G, Franklin, KBJ. The Mouse Brain in Stereotaxic Coordinates 2nd Edition. Academic Press; San Diego: 2001.

Pinto L, Goard MJ, Estandian D, Xu M, Kwan AC, Lee S-H, Harrison TC, Feng G, Dan Y. 2013; Fast modulation of visual perception by basal forebrain cholinergic neurons. Nat Neurosci. 16:1857–1863. [PubMed: 24162654]

Purushothaman G, Marion R, Li K, Casagrande VA. 2012; Gating and control of primary visual cortex by pulvinar. Nat Neurosci. 15:905–12. [PubMed: 22561455]

Rieck R, Carey RG. 1984; Evidence for a laminar organization of basal forebrain afferents to the visual cortex. Brain Res. 297:374–380. [PubMed: 6722546]

Roberts MJ, Zinke W, Guo K, Robertson R, McDonald JS, Thiele A. 2005; Acetylcholine dynamically controls spatial integration in marmoset primary visual cortex. J Neurophysiol. 93:2062–72. [PubMed: 15548624]

Roth MM, Dahmen JC, Muir DR, Imhof F, Martini FJ, Hofer SB. 2016; Thalamic nuclei convey diverse contextual information to layer 1 of visual cortex. Nat Neurosci. 19:299–307. [PubMed: 26691828]

Sanderson KJ, Dreher B, Gayer N. 1991; Prosencephalic connections of striate and extrastriate areas of rat visual cortex. Exp Brain Res. 85:324–334. [PubMed: 1716594]

Sarter M, Hasselmo ME, Bruno JP, Givens B. 2005; Unraveling the attentional functions of cortical cholinergic inputs: interactions between signal-driven and cognitive modulation of signal detection. Brain Res Brain Res Rev. 48:98–111. [PubMed: 15708630]

Seabrook TA, Burbridge TJ, Crair MC, Huberman AD. 2017; Architecture, function, and assembly of the mouse visual system. Annu Rev Neurosci. 40:499–538. [PubMed: 28772103]

Sillito AM, Kemp JA. 1983; Cholinergic modulation of the functional organization of the cat visual cortex. Brain Res. 289:143–55. [PubMed: 6661640]

Stepniewska I, Kaas JH. 1997; Architectonic subdivisions of the inferior pulvinar in New World and Old World monkeys. Vis Neurosci. 14:1043–60. [PubMed: 9447687]

Tigges J, Tigges M, Cross NA, McBride RL, Letbetter WD, Anschel S. 1982; Subcortical structures projecting to visual cortical areas in squirrel monkey. J Comp Neurol. 209:29–40. [PubMed: 7119172]

Tohmi M, Meguro R, Tsukano H, Hishida R, Shibuki K. 2014; The extrageniculate visual pathway generates distinct response properties in the higher visual areas of mice. Curr Biol. 24:587–97. [PubMed: 24583013]

Van Hooser SD, Nelson SB. 2006; The squirrel as a rodent model of the human visual system. Vis Neurosci. 23:765–778. [PubMed: 17020632]

Vanni MP, Thomas S, Petry HM, Bickford ME, Casanova C. 2015; Spatiotemporal profile of voltage-sensitive dye responses in the visual cortex of tree shrews evoked by electric microstimulation of the dorsal lateral geniculate and pulvinar nuclei. J Neurosci. 35:11891–11896. [PubMed: 26311771]

Wickersham IR, Lyon DC, Barnard RJO, Mori T, Finke S, Conzelmann K-K, Young JaT, Callaway EM. 2007; Monosynaptic restriction of transsynaptic tracing from single, genetically targeted neurons. Neuron. 53:639–47. [PubMed: 17329205]

Wong P, Kaas JH. 2008; Architectonic Subdivisions of Neocortex in the Gray Squirrel (*Sciurus carolinensis*). Anat Rec Adv Integr Anat Evol Biol. 291:1301–1333.

Wong P, Kaas JH. 2010; Architectonic Subdivisions of Neocortex in the Galago (Otolemur garnetti). Anat Rec Adv Integr Anat Evol Biol. 293:1033–1069.

Xu X, Ichida JM, Allison JD, Boyd JD, Bonds AB, Casagrande VA. 2001; A comparison of koniocellular, magnocellular and parvocellular receptive field properties in the lateral geniculate nucleus of the owl monkey (Aotus trivirgatus). J Physiol. 531:203–18. [PubMed: 11179404]

Zhou NA, Maire PS, Masterson SP, Bickford ME. 2017; The mouse pulvinar nucleus: Organization of the tectorecipient zones. Vis Neurosci. 34:E011. [PubMed: 28965504]

Zhou N, Masterson S, Damron J, Guido W, Bickford M. 2018; The mouse pulvinar nucleus links the lateral extrastriate cortex, striatum, and amygdala. J Neurosci. 38:347–362. [PubMed: 29175956]

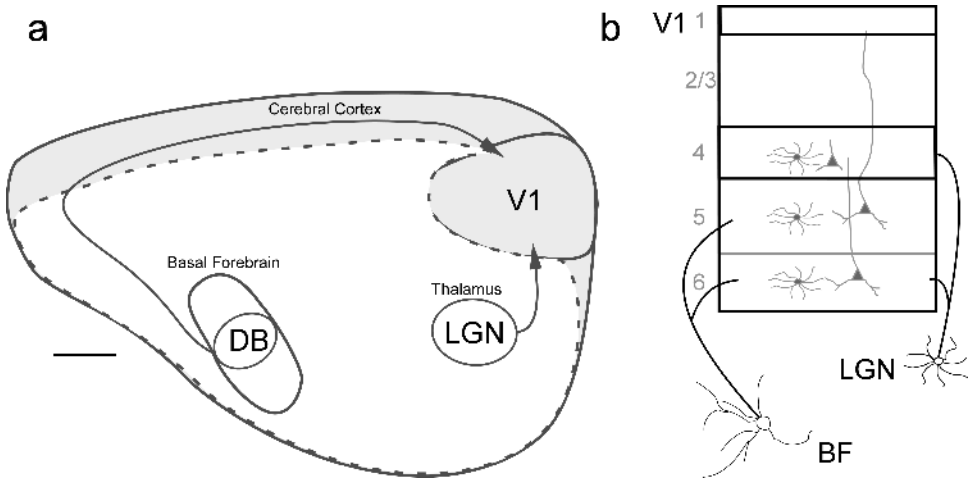

Figure 1.

Schematic of basal forebrain projection to mouse V1. (a) The basal forebrain (BF) projects to V1 from neurons located in the diagonal band (DB) region. V1 input from the lateral geniculate nucleus (LGN) of the thalamus is also indicated. Scale bar equals 1 mm. (b) Basal forebrain inputs terminate in layers 5 and 6; LGN inputs terminate primarily in layers 4 and 6.

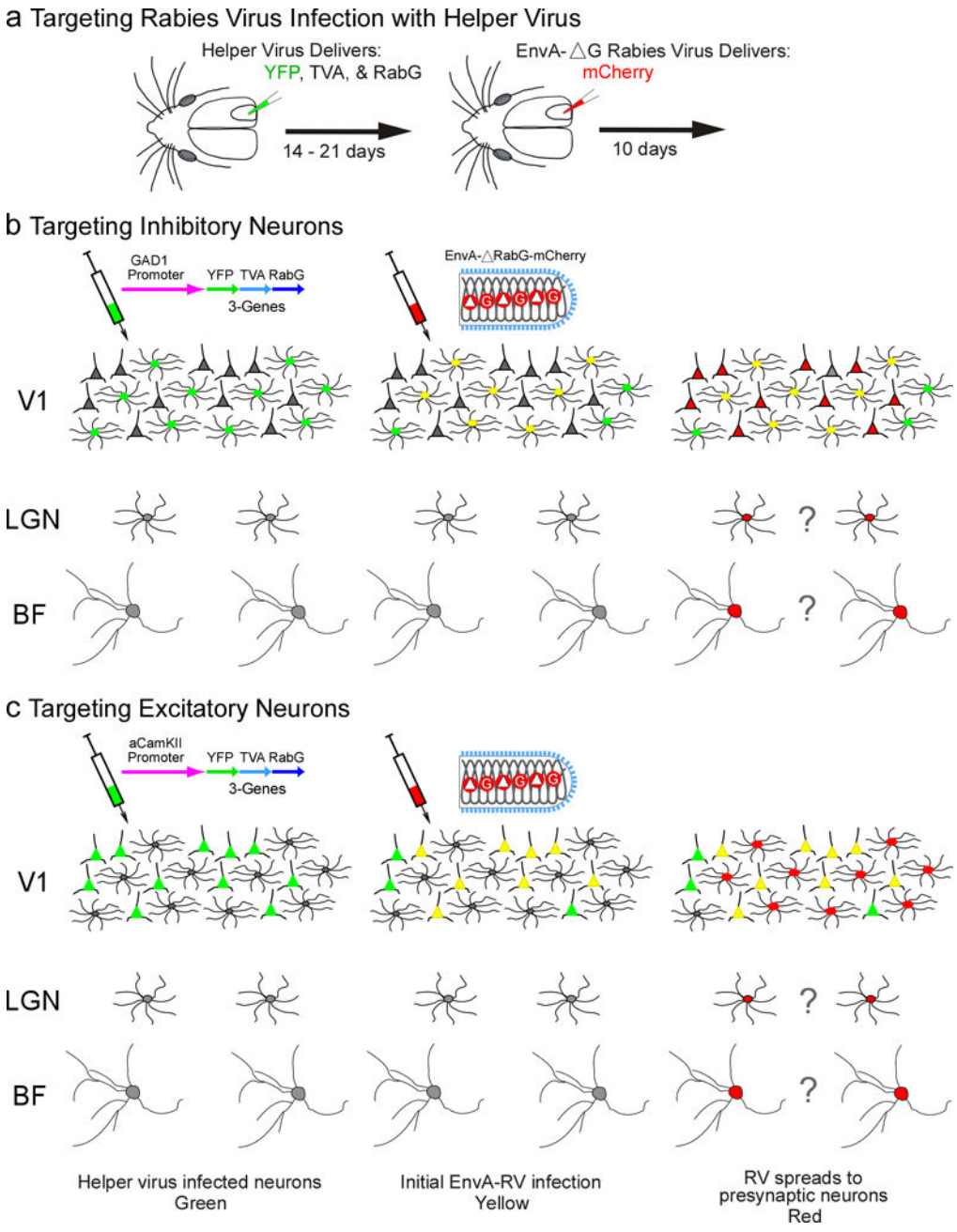

Figure 2.

Cell type specific tracing schematic. (a) Helper virus is used to deliver three genes (YFP, TVA, and RabG) to a local population of neurons in mouse V1 (left). Following a 2–3 week survival period, EnvA-ΔG -RV which will express mCherry in infected neurons is injected into the same V1 location (right). The RV injection is followed by a 10 day survival period. (b and c) (Left) Helper virus cell type specificity is achieved with the GAD1 (a) or αCamKII (c) promoter. In this way the YFP reporter (green) will express only in V1 inhibitory (b) or excitatory pyramidal (c) neurons. (Middle) EnvA-ΔG-RV can only infect neurons expressing the TVA receptor, the second gene product of the helper virus. Resulting super-infected neurons are identified by co-expression of YFP and mCherry (yellow). (Right) Expression of

the RabG, the third helper virus gene product, is incorporated into the ΔG-RV-mCherry produced within super-infected neurons (starter cells; yellow) enabling RV to infect presynaptically connected neurons (red). Whether or not basal forebrain neurons provide direct synaptic inputs to inhibitory and excitatory neurons is the question (?) being investigated here.

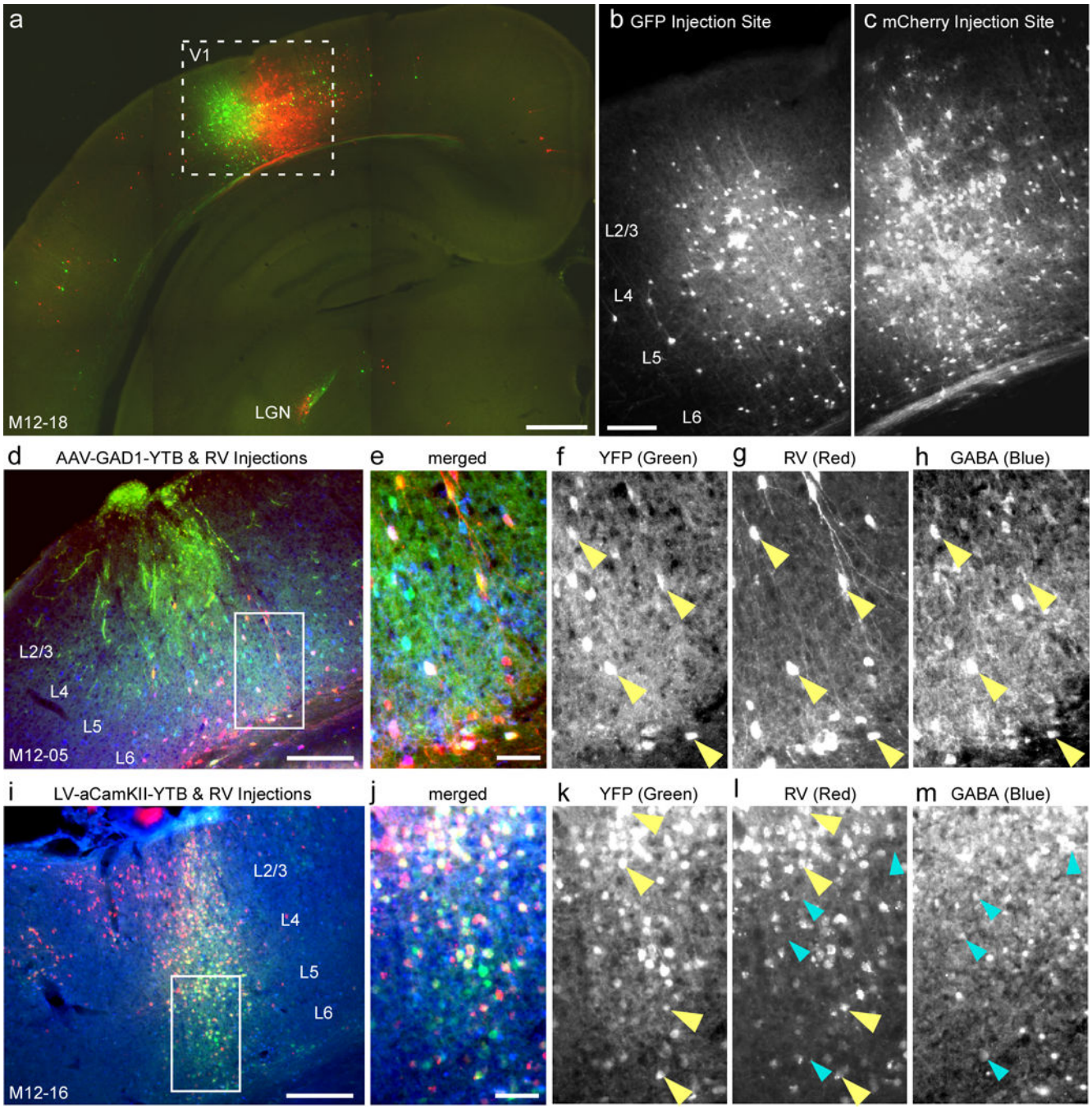

Figure 3.

Digital images of virus injection sites in V1. (a) Injections of ΔG-GFP (green) and ΔG-mCherry (red) are shown side-by-side in case M12–28. (b, c) Higher magnification digital images of the same GFP (b) and mCherry (c) ΔG-RV are shown in black and white and indicate that injection sites extended through layers 4–6. (d) Injection sites of AAV-GAD1-YTB expressing YFP (green) and EnvA-ΔG-RV expressing mCherry (red) are shown in a section through V1 processed for the GABA antibody (blue) in case M12–05. (e-h) Higher magnification images of the layer 5/6 region outlined by the white rectangle in (d).

Inhibitory starter cells co-expressing YFP (f) and mCherry (g) are positive for the GABA antibody (h); for reference a portion of starter cells are identified by yellow arrowheads. (i) Injection sites of LV-αCamKII-YTB expressing YFP (green) and EnvA-ΔG-RV expressing mCherry(red) are shown in a section through V1 processed for the GABA antibody (blue) in case M12–16. (j-m) Higher magnification images of the layer 5/6 region outlined by the white rectangle in (I). Excitatory starter cells co-expressing YFP (k) and mCherry (l) are negative for the GABA antibody (h); a sample of starter cells are identified by yellow arrowheads; a sample of GABA-positive neurons are marked by blue arrowheads. Scale bars in (a, d, and i) equal 200 μm; Scale bars in (b, e, and j) equal 50 μm.

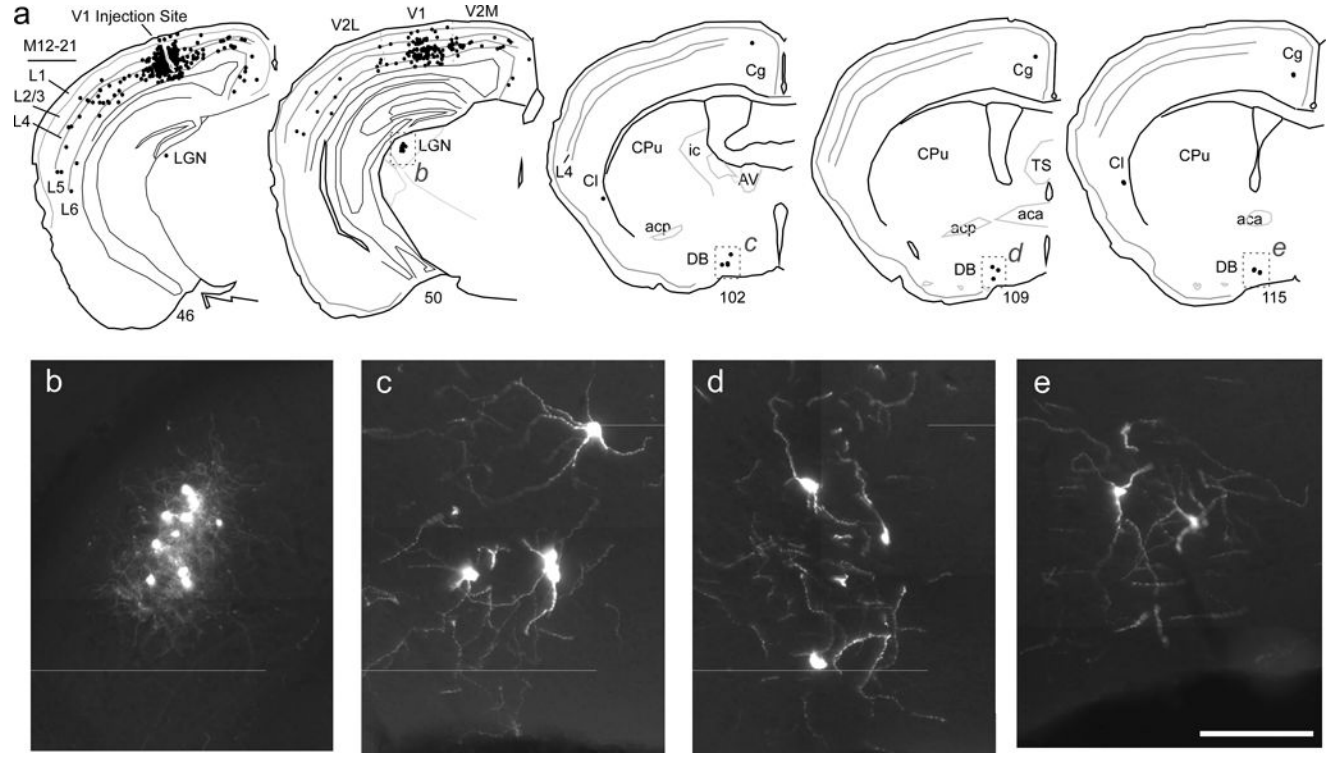

Figure 4.

Retrogradely infected neurons in the diagonal band of the basal forebrain following V1 injection of ΔG-RV. (a) A reconstruction of the pattern of rabies virus infected neurons (black dots) in 5 coronal sections presented from posterior (section 46) to anterior (section 115) in case M12–21. The V1 injection site is shown in section 46. Scale bar equals 1 mm. (b-e) Digital images of rabies virus infected neurons in the LGN (b) and diagonal band of the basal forebrain (c–e) from regions corresponding to dashed rectangles in (b). Scale bar equals 200 μm.

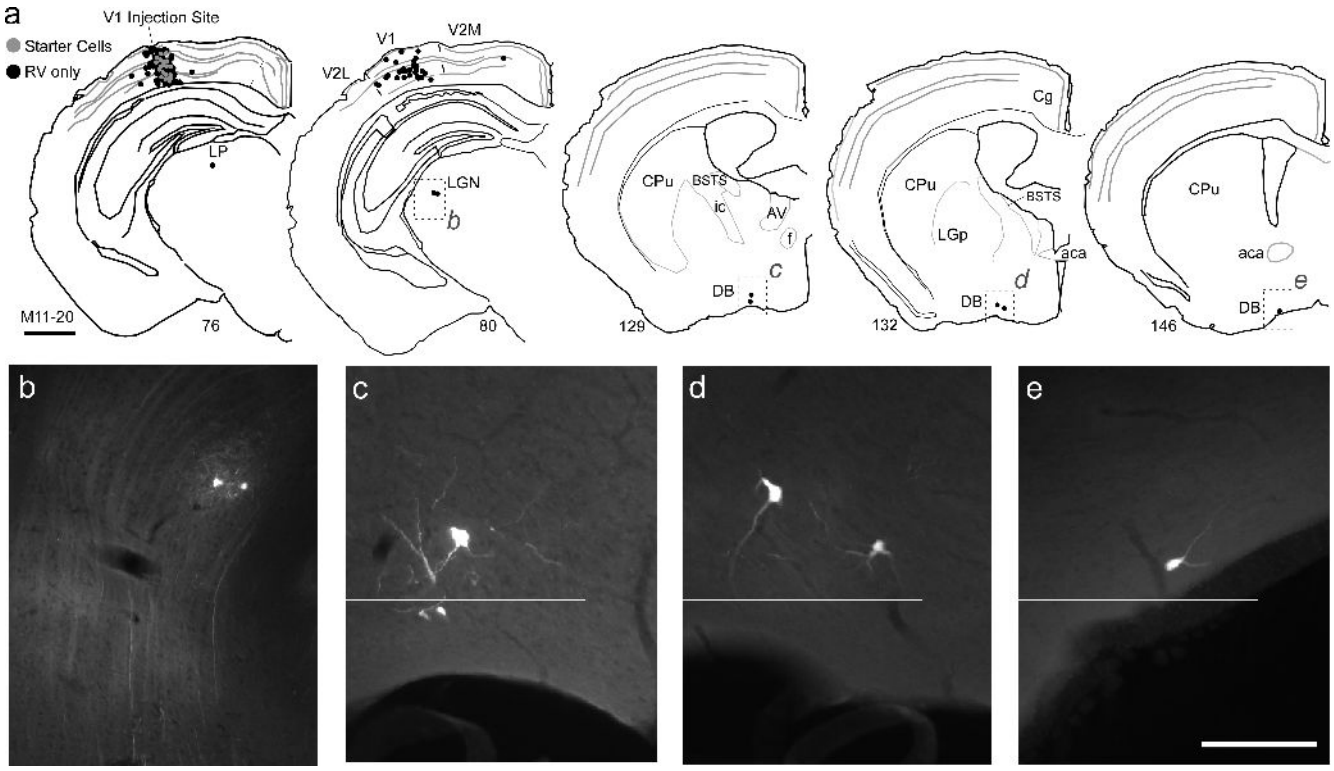

Figure 5.

Basal forebrain neurons project directly to V1 inhibitory neurons. (a) V1 inhibitory starter cells (gray dots) shown at the injection site in section 76, resulted from injection of AAV-GAD1-YTB followed three weeks later by injection with EnvA-ΔG-RV (see Figure 2a,b). Presynaptic inputs to inhibitory starter cells are also shown (black dots). (b–e) Digital images of rabies virus infected neurons in the LGN (b) and diagonal band of the basal forebrain (c–e) from regions outlined by dashed rectangles in (a). Other conventions as in Figure 4.

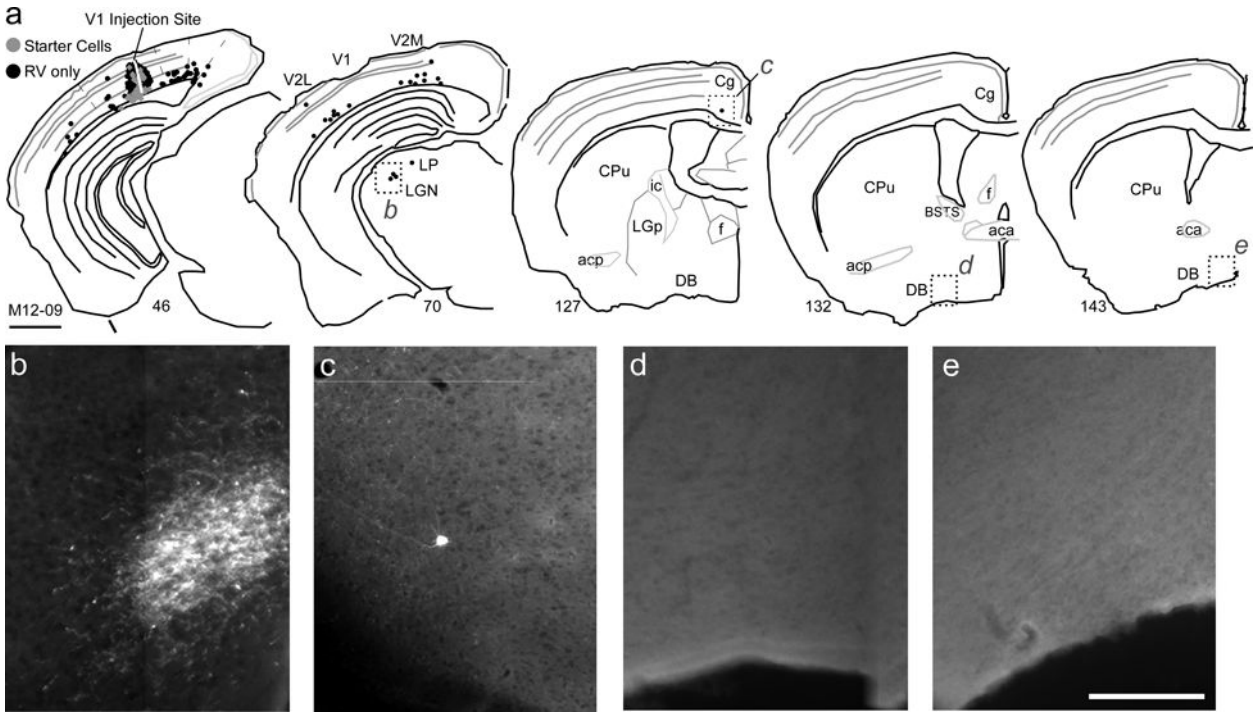

Figure 6.

No evidence for direct basal forebrain inputs to V1 excitatory neurons. (a) Excitatory starter cells (gray dots) shown at the injection site in section 45, resulted from injection of LV-αCamKII-YTB followed three weeks later by injection with EnvA-ΔG-RV (see Figure 2a,c). Presynaptic inputs to excitatory starter cells are also shown (black dots). Scale bar equals 1 mm. (b–e) Digital images of the regions outlined in (a). Rabies virus infected neurons were found in the LGN and cingulate cortex, but not in the basal forebrain (d and e). Other conventions are as in Figure 4.

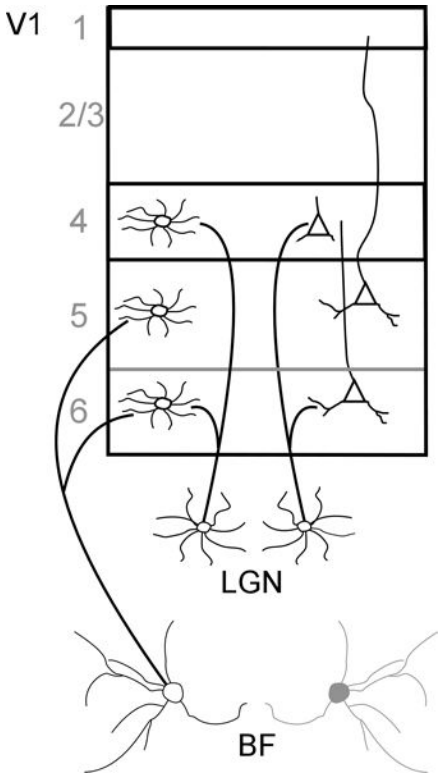

Figure 7.

Summary of cell type specific basal forebrain input to V1. Based on the results from our dual viral tracing method, V1 inhibitory neurons receive direct inputs from the basal forebrain and LGN; whereas V1 excitatory neurons receive direct input from the LGN but not the basal forebrain.

Table 1

Number of retrogradely infected neurons in the diagonal band and LGN following glycoprotein deleted rabies virus injections in mouse V1.

Case No.	Rabies Virus	Diagonal Band	LGN
M12–13	ΔG-GFP	2	3
M12–13	ΔG-mCh	3	3
M12–21	ΔG-mCh	51	52
M12–22	ΔG-mCh	8	16
M12–27	ΔG-mCh	6	6
M12–28	ΔG-GFP	11	42
M12–28	ΔG-mCh	14	45
M12–29	ΔG-GFP	14	10
M12–29	ΔG-mCh	12	15

Table 2

Number of retrogradely infected neurons in the diagonal band and LGN projecting to V1 starter cells in Layers 4, 5, and 6.

Case No.	Helper Virus	Starter Cell Type	Starters No.: Layer 4	Layer 5	Layer 6	Diagonal Band	LGN
M11–16	AAV-GAD1	Inhibitory	35	3	1	0	16
M11–20	AAV-GAD1	Inhibitory	3	14	13	23	22
M12–05	AAV-GAD1	Inhibitory	7	22	34	6	2
M12–06	AAV-GAD1	Inhibitory	4	17	39	13	7
M12–07	AAV-GAD1	Inhibitory	6	42	28	2	0
M12–17	AAV-GAD1	Inhibitory	9	44	24	4	32
M11–19	LV-αCamKII	Excitatory	6	16	22	0	4
M12–09	LV-αCamKII	Excitatory	3	48	38	0	8
M12–10	LV-αCamKII	Excitatory	2	12	26	0	0
M12–15	LV-αCamKII	Excitatory	32	53	60	0	12
M12–16	LV-αCamKII	Excitatory	13	16	13	0	4
M12–26	LV-αCamKII	Excitatory	8	11	4	0	4